Egypt.J.Chem. **Vol. 63**, No. 3. pp. 953-960 (2020)

Egyptian Journal of Chemistry
http://ejchem.journals.ekb.eg/

Excited-State Deactivation Pathways of 7-Mercapto-4-Methyl-Coumarins: Theoretical Insight

M. S. A. Abdel-Mottaleb
Computational Chemistry Laboratory, Department of Chemistry, Faculty of Science, Ain Shams University, 11566 Abbassia, Cairo, Egypt.

EXPERIMENTALLY reported photophysics of 7-mercapto-4-methyl coumarin compounds in methanol (thiol (C-SH) and thione (C=S)) disclose that these materials are weak or non-fluorescent. When the thiol is methylated, the C-S(CH_3) material shows strong fluorescence. This work focuses on applying two computational strategies based on DFT and its time-dependent extension TD-DFT to validate the experimental findings. On-the-fly single reference TDDFT computational is first applied, which identified in a simple way that the S_1/S_0 intersection is the main radiationless channel leading to fluorescence quenching in mercapto derivatives. A second supporting method based on scanning along of C-S bond distance in the S_0 and S_1 states is used. Both strategies came to similar conclusions. The applied approaches introduce quantitative explanation of the mechanism of radiationless deactivation in mercapto coumarins due to S_1/S_0 conical intersection (CI) or due to small S_1/S_0 energy gap in case of thione tautomer, which is the dominant (thermodynamically favorable) tautomer in the S_1 state. The results of this insights may assist designing profitable new fluorescent or non-fluorescent materials by changing specific functional group(s) in the molecule.

Keywords: Conical intersection, Fluorescence, Tautomers, TD-DFT, Thiol, Thione.

Introduction

Due to its practical significance as well as pivotal and diverse applications in many fields of biological, medicinal and industrial importance, several studies have been carried out to investigate spectroscopic, electronic structures, solvatochromic behaviour and photophysical properties of coumarin derivatives such as 7-hydroxy-4-methylcoumarin (4-methylumbelliferone); [1-5] and some other coumarins [6-9]. Recently, some mercapto coumarins; namely 7-mercapto-4-methyl coumarin compounds (thiol (C-SH) and thione (C=S)) [10-12] with appealing photochemical and photophysical properties have been studied.

Density functional theory (DFT) and its time-dependent (TD) extension TD-DFT quantum mechanical computations of vertical and adiabatic excitations of neutral, deprotonated and protonated forms of coumarins have been reported in the gas and liquid phases [13-17]. Theoretical computational methods are powerful tool for molecular design and can help explicit identification of molecular characteristics and reactivities as well as the spectroscopic features in the ground and excited states of molecules of potential applications and in validating experimental results in a non-expensive way.

Recent published work reports on the photophysical properties of 7-mercapto-4-methylcoumarin in protic and non-protic solvents [10]. In spite of their potential applications as optical whitening agents, only few publications reported the fluorescent 7-mercaptocoumarin derivatives [11, 12]. Interestingly, 7-hydroxy-4-methyl-coumarin and its tautomers show strong fluorescence, while the replacement of the hydroxyl group by a thiol in case of molecule (1), makes C-SH poorly fluorescent. This is due to its thione-like C=S tautomeric form (2). It is also reported that the alkylation of the thiol group (3) appears to retrieve the fluorescence properties of the coumarin moiety [10]. The origin and character of the lowest singlet states are qualitatively discussed before [10], specifically proposing, in a hypothetical way that the thione-like C=S resonance form (2) plays a key role in excited state deactivation in C-SH (1).

Corresponding author e-mail: fm.s.abdelmottaleb@sci.asu.edu.eg ORCID ID: 0000-0003-3462-2396
Received 30 /6/2019; Accepted 5/8/2019
DOI: 10.21608/ejchem.2019.14179.1874

In view of the paucity of information related to mercapto coumarins, the main goal of this work is to check, in a non-expensive approach, whether on-the-fly TDDFT dynamics of the mercapto coumarin molecules could validate radiationless deactivation of the S_1 state through conical intersections (CI) among the potential energy surfaces (PES) of the singlet states (S_1/S_0 CI) leading to the observed weak fluorescence due to the thione dominant tautomer (2). However, the advantages and drawback features of single reference TD-DFT methods were discussed before [18-23]. Thus, it will be interesting to check the theoretical insights for mercapto-coumarins by using single-reference TD-DFT simulations. In particular, relaxed scans will be performed along normal modes as well as along constrained C-S bond distance. In case that the proposed S_1/S_0 CI or S_1/S_0 energy gap value is rightly responsible for weak or non-fluorescent molecules via radiationless deactivation, almost similar PESs obtained by the two approaches should be expected.

Additionally, computed thermodynamic stability parameters such as enthalpy (Hand Gibbs free energy (Gof the studied molecules in their S_0 and S_1 states will be investigated to verify the stabilities of the tautomers (1) and (2).

Methods

The calculations considered the molecules shown in Fig. 1. Ground-state (S_0) geometries were optimized using the DFT method with the range-separated hybrid functional ωB97X-D that includes empirical corrections for long range non-bonded dispersive interactions and basis set 6-311G (d,p), which is a recommended method for geometries including molecules incorporating transition metals. CIS/6-31G(d) method was used for computing thermodynamics data in the S1 state. Single point calculations were performed with the same method to compute thermodynamic parameters. Spartan'18 parallel software with its user-friendly built-in GUI was used [24]. It generates a list of tautomers in an easy way.

ORCA (parallel) package 4.0.1 [25-27] was used for computing vertical electronic transitions from S_0 equilibrium geometry to S_1 state (absorption transition) and from S_1 equilibrium geometry to the ground state (fluorescence). Geometry optimization of molecules studied in their S_0 state at ωB97X-D/6-311G(d,p) [28] and S_1 state at TD-DFT employing CAM-B3LYP/6-311G(d,p) levels of the theory [29] are computed. CAM-B3LYP/6-311G(d,p) results are in good agreement with the experimental results available in the literature [10]. Long-range corrected hybrid density functional includes empirical damped atom-atom dispersion corrections ωB97X-D and the hybrid exchange–correlation functional using Coulomb-attenuating method CAM-B3LYP are of significant accuracy.

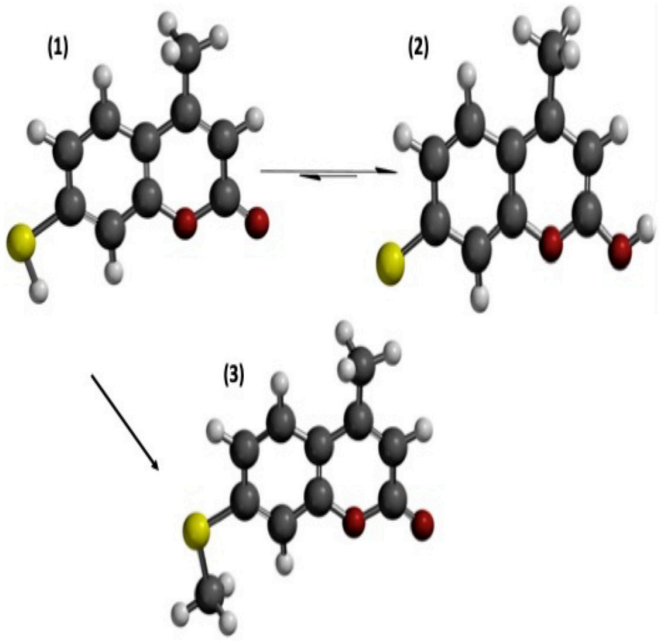

Fig. 1. The schematic structure (Optimized) of molecules under investigation (1-3) [atom colour: C, H, O, and S are dark grey, white, red and yellow, respectively].

ORCA outputs are visualized by using ChemCraft GUI (ChemCraft.com). No imaginary frequencies were obtained by carrying out frequency calculations in the ground and the excited states in the gas phase as well as in methanol indicating that the molecules are at minima. ORCA enabled us to carry out potential energy surface (PES) scans along normal coordinates of IR modes. The output of the "trajectory" run automatically contains the excited state energies in addition to the ground state energy. The output file from this job contains the total energies (i.e. the ground state energy plus the excitation energy) for each excited state as a function of displacement of the chosen normal mode.

First, we ran an optimization-frequency job using ωB97X-D/def2-SV(P) and auxiliary basis def2/J to accelerate generation of the nuclear Hessian matrix. The Hessian matrix was used to construct normal mode trajectories. This is followed by using single reference TD-DFT scan calculations for a range of the displaced geometries (q). Furthermore, scanning along C-S bond distance was performed using Spartan'18 parallel suite with its built-in user-friendly GUI. In steps scans of C-S bond distance (constrained distance) using ωB97X-D/631-G(d) and CIS/631-G(d) give potential energy surfaces (PESs) of the molecules in S_0 and S_1 states, respectively.

A Broadberry workstation (40 cores) (UK) and a Mac Pro (12 core) workstation were used.

Results and Discussion

Absorption and fluorescence properties

Table 1 contains experimental and theoretical absorption and fluorescence parameters. Experimental parameters are reported in the literature [10]. The spectroscopic parameters are computed using TDDFT/CAM-B3LYP/311G(d,p) model as implemented in ORCA package. Generally, inspection of Table 1 reveals the good agreement between our computed data with the available experimental results collected from the literature. Accurate quantum mechanical calculations point to the CT nature of the electronic transitions. Molecular orbitals mainly involved in the electronic transitions are represented in Fig. 2. Closer look reveals the charge transfer nature of the electronic transitions (mainly from the HOMO-1 and/or HOMO to LUMO transition). Interestingly, HOMO-1 → LUMO CT transition occurs in (1) and (3). In (2) HOMO → LUMO transitions are of nature, while HOMO-1 → LUMO in (2) is a forbidden transition because HOMO-1 orbitals are of nature and perpendicular to LUMO () positioned on the plane of the planar molecules.

Interestingly, it has been reported that thiol (1) is weakly or non-fluorescent in methanol or water, respectively. However, the alkylation of the thiol group (3) seems to recover the fluorescence properties of the coumarin [10] as shown in Table 1 where the experimental fluorescence quantum yield of (3) , is about 53 times higher than that of (1). Very high non-radiative rate constant (k(non-rad)/ns^{-1}) was determined experimentally in case of (1) [10] and given in Table 1. It decreased substantially in case of (3). The origin and character of the lowest singlet states are discussed before [10], specifically proposing in a descriptive way that the thione-like C=S resonance form plays a key role in excited state deactivation in C-SH. Our theoretical results (Table 1.) confirm the reported result of the fluorescence of (1) at pH 2.0 [10], which is likely originated from tautomer (2) [10].

Molecular thermodynamics

Thermodynamic parameters are summarized in Table 2. The results listed in Table 2 reveal the following thermodynamic trends:

i) Relative total energy in the S_0 state, relative H^0 and G^0 values decrease in the order (1) > (2). Relative to the thiol (1), the thione form (2) is destabilized (positive relative energy value as well as positive other thermodynamic parameters) reflecting its enhanced electronic sensitivity to the medium. In the S_1 state, (2) is more favorable than (1).

ii) $\Delta G_{1,2} = (G^o_1 - G^o_2) = -83$ kJ/mol. The results provide further support favoring thione stability over the corresponding thiol tautomer. It means that in the S_1 state tautomerization of thiol (1) to thione (2) is a spontaneous process.

Interestingly, excited state proton transfer (ESPT) should be facilitated because thione is energetically more stable than its thiol tautomer in S_1 state. This is in agreement with similar results reported before for keto-enol in 4-methyl-7-hydroxy coumarin [17]. Thus, thione tautomer is the one from which the relaxation of S_1 to the ground state predominantly happens.

TABLE 1. Computed spectroscopic parameters[1)] of the studied molecules (available experimental values in methanol[2)] are given between parentheses[2)]). Orca codes were used.

Molecule	uv/nm	f(abs)	flu/nm	Φf	k(non-rad)/ns^{-1}
(1)	318.4 (326)	0.440	338.8 (340)	0.01	>9.9
(2)	387.8	0.014	400.3(~ 400)[3)]		
(3)	332.0 (333)	0.439	350.0 (411)	0.53	0.25

[1)]Major contributions (95.5%) are from HOMO→LUMO
(See Figure 2. for some important M.O. surfaces (of 0.002 isovalue) of different molecules studied).
[2)]Experimental values between parentheses and , k(non-rad) are from [10]
[3)]Fluorescence spectrum of (2) at pH 2.0 (aqueous solution) from [10]

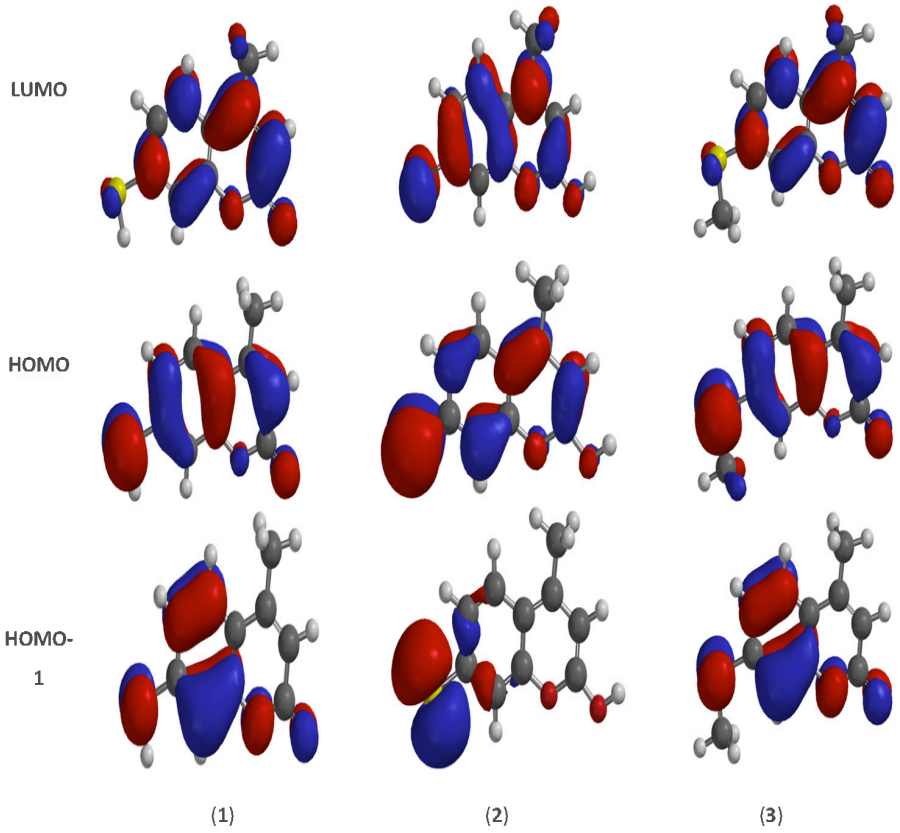

Fig. 2. MO's of molecules (1)-(3) included mainly in the electronic transitions (their energies in eV are given in Table 2). See text. The nature of the electronic transition of all molecules is * transition. HOMO-1 to LUMO transition in (2) is forbidden (orthogonal orbitals).

TABLE 2. Relative energies and molecular thermodynamic parameters in the S_0 and S_1 of molecules studied using (ωB97X-D /6-31G(d) and (CIS/6-31G(d))methods, respectively, CPCM:Methanol model using Spartan'18 Parallel package).

Molecule	Rel. E (kJ/mol)		Rel. H° (kJ/mol) In S_0	Rel. G° (kJ/mol) In S_0	E^{HOMO} (eV)	E^{LUMO} (eV)
	S_0	S_1				
(1)	0.0	0.0	0.0	0.0	-7.99	0.06
(2)	130.44	-94.6	99.7	99.8	-7.13	-0.84
(3)	---	---	--	--	-7.79	0.10

Potential energy surface (PES) scans along normal coordinates

The adiabatic potential energy surfaces scan as a function of normal coordinate displacement are obtained from on-the-fly high-level TDDFT calculations to examine the S_1/S_0 intersection on the PESs of thione tautomer (2) in methanol using ORCA package. These calculations are nevertheless very helpful in obtaining at least a rough idea about excited state energy surfaces.

PES of different ground and excited states were obtained by scanning along normal coordinates of the chosen IR mode. The results of PES obtained for thiol (1), thione (2) tautomers and -S(CH_3) derivative (3) are depicted in Fig. 3. We selected the IR mode that involves almost all atoms in the molecules with largest contribution from the C-S bond bonding vibration. Figure 3 reveals apparent S_1/S_0 intersection in case of the weakly-fluorescent thione tautomer (2) at q=3.2. Passage through this apparent intersection on the PES computed in methanol leads to nonradiative energy dissipation due to molecular dynamics. However, this explains the non-fluorescence of thione tautomer.

It is obvious that tautomerization of the C-SH (1) to thione (2) results in radiationless deactivation of its S_1 state due to crossing the point of intersection with the PES of S_0. The fluorescence is restored by replacement of C-SH (1) by C-S(CH_3) in molecule (3) because the PESs position further apart from each other relative to PESs of (3), and thus reduces the probability of radiationless energy dissipation in (3). Our results quantitatively explain the experimental findings reported in [10]. It is worth to mention that S_1/S_0 intersection does not exist in PESs computed in gas phase where the S_1 PES places normally higher than that of S_0. This is in consistence with the experimentally noticed fluorescence-induced changes in different solvents [10].

An alternative way to construct PESs in S_0 and S_1, is to perform relaxed scan along C-S bond distance constrain. Figure 4 shows the results for the molecules (2) and (3). Very good agreement between the results obtained by the two different approaches is observed (compare Fig. 3 and Fig. 4). Both approaches support each other and leading to the same conclusion that non-radiative pathway is achieved either via S_1/S_0 CI (obtained by scanning along vibrational modes mostly include C-S bond displacement) or the noticed smaller S_1/S_0 energy gap (Fig. 4) in case of (2), which renders it non-fluorescent material.

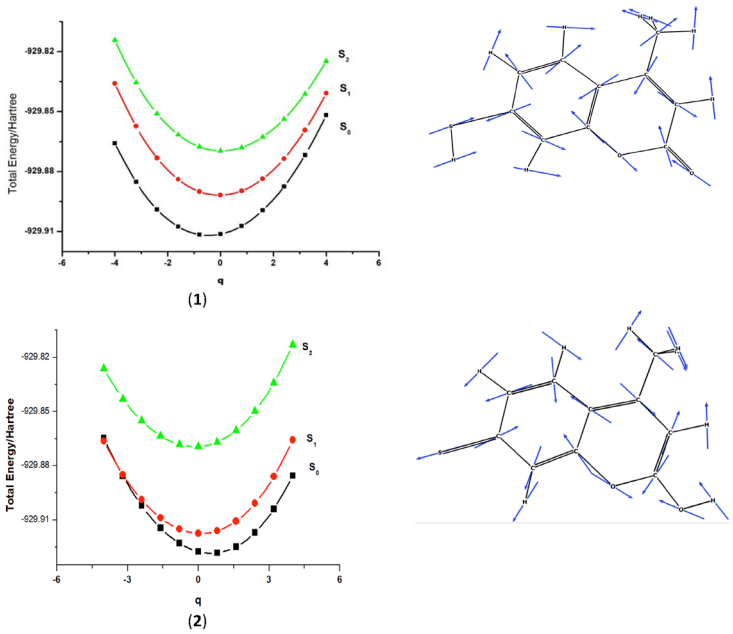

Fig. 3. (Left side) PES along the displacement coordinate (q) of the thiol tautomer (1), its thione (2) tautomer and C-S(CH_3) derivative (3) (in methanol) of the chosen IR mode in cm^{-1} that takes place at 1137.6 (1), 1146.5 (2) and 1008.3 (3) [displacement vectors are visualized at right-side). The IR mode at 1146.5 cm^{-1}, in the ground state computed IR spectrum, involves almost all atoms and bonds in the molecules, particularly the C=S thione tautomer (2).

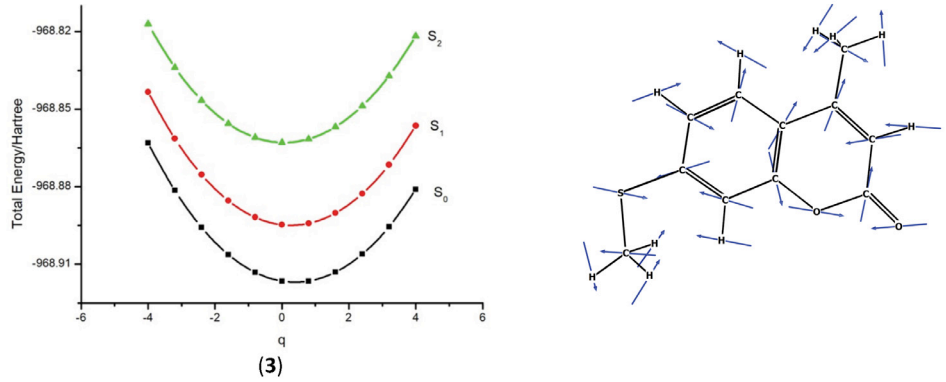

Fig. 3

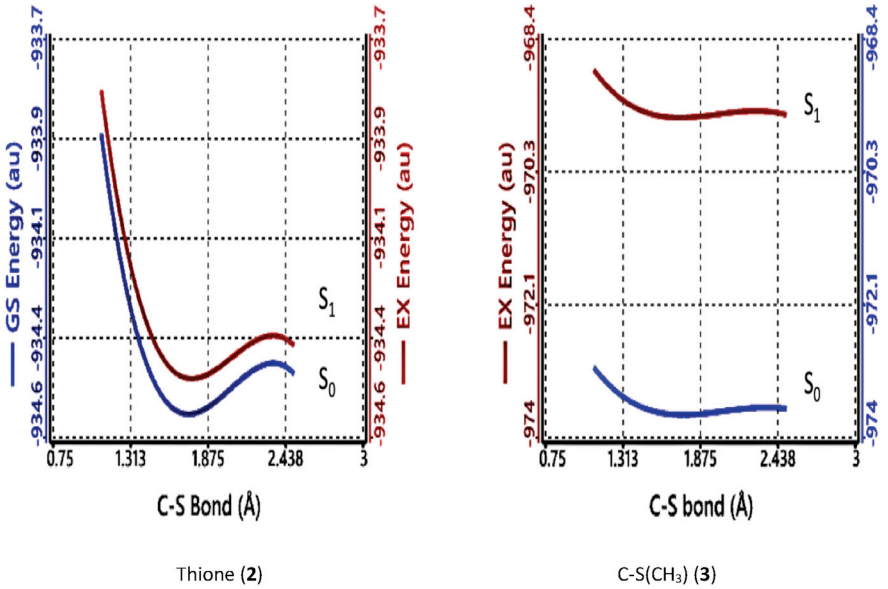

Thione (**2**) C-S(CH_3) (**3**)

Fig. 4. Relaxed scan along C-S constrained bond distance. Smaller S_1/S_0 gap in thione renders it non-fluorescent due to extensive non-radiative deactivation of S_1 state. Same results have been obtained using ORCA package.

It is well understood that the used on-the-fly single reference TD-DFT computational methodology cannot describe the CI topology (the slopes of the intersecting cones around the degenerate structures). The advantages and drawback features were discussed before [18-24]. However, using such a single-reference method, which is inexpensive computational methodology, could be considered as a simplified approach to locate conical intersections, at least in an approximate way, and explains the experimental findings. Obviously, exact location of CI would require a multireference CASSCF computations [30-32] with large active spaces. This requisite can be a significant hindrance when executing excited state dynamics, since application of multireference methods can have prohibitively high computational cost. Moreover, there is possibility that the most appropriate active space may change along a PES.

Conclusion

This paper focused on simulating electronic, optical, and thermodynamic properties of 7 -mercapto - 4 - methyl -coumarin using DFT and TD -DFT. Thermodynamic parameters have been computed and reveal the greater stability of the thione form in the S_1 state. The calculations verified the experimentally available spectroscopic data.

Similar PESs are obtained by two computational approaches: 1- relaxed scan along normal vibrational mode that mainly relevant to C-S bond and 2- relaxed scan along C-S constrained bond distance. On the basis of a simply computed on-the-fly adiabatic PES of different

singlet states, we have identified crossing point between S_1 and S_0 states, in case of thione, which realizes non-radiative relaxation, in agreement with the lack of its fluorescence reported before [10]. Relaxed scan along C-S bond distance leads to similar supportive conclusion.

The results of this theoretical study may assist designing profitable new fluorescent or non-fluorescent materials by changing specific functional group(s) in the molecule.

Conflicts of Interest

There are no conflicts to declare.

Computational data are available upon request.

References

1. Abdel-Mottaleb, M. S. A., El-Sayed, B. A., Abo-Aly, M. M., El-Kady, M. Y. Fluorescence-properties and excited state interactions of 7-hydroxy-4-methylcoumarin laser dye. *J. Photochem. Photobiol. A, Chem.* **46**, 379-390 (1989).
2. Jones, G. , Jimenez, J. A. C. Azole-linked coumarin dyes as fluorescence probes of domain-forming polymers. *J. Photochem. Photobiol B.* **65**, 5-12 (2001).
3. Bangar Raju, B., Costa, S. M. B. Excited-state behavior of 7-diethylaminocoumarin dyes in AOT reversed micelles: Size effects. *J. Phys. Chem. B.* **103**, 4309-4317 (1999).
4. DeSilva, N., Minezawa, N., Gordon, M. S. Excited-state hydrogen atom transfer reaction in solvated 7-hydroxy-4-methylcoumarin. *J. Phys. Chem. B.* **117**, 15386-15394 (2013).
5. Kaholek, M., Hrdovie, P. Spectral properties of coumarin derivatives substituted at position 3. Effect of polymer matrix. *J. Photochem. Photobiol. A.* **108**, 283-288 (1997).
6. Yamada, Y., Okamoto, M., Kikuzaki, H., Nakatani, N. Spasmolytic activity of auraptene analogs. *Biosci. Biotechnol. Biochem.* **61**, 740-742 (1997).
7. Excited-State Reactions of Coumarins in Aqueous Solutions. III. The Fluorescence Quenching of 7-Ethoxycoumarins by the chloride ion in acidic solutions. *Bull, Chem. Soc. Jpn.* **59**, 961-968 (1986).
8. Kumar, S., Giri, R., Machwe, M. K. Effect of substituent on intramolecular charge transfer and excited state dipole moments of amino coumarins, *Ind. J. Pure Appl. Phys.* **36**, 622-626 (1998).
9. Nielsen, B. E. Coumarins patterns in the Umbrelliferae, In: "T*he Biology and Chemistry of the Umbrelliferae*", Heywood, V. H. (Ed.); Academic Press, London (1971).
10. Lanterna, A. E., González-Béjar, M., Frenette, M., Scaiano, J. C. Photophysics of 7-mercapto-4-methylcoumarin and derivatives: complementary fluorescence behaviour to 7-hydroxycoumarins. *Photochem. Photobiol. Sci. RSC.* **16**, 1284-1289 (2017).
11. González-Béjar, M., Frenette, M., Jorge, L., Scaiano, J. C. 7-Mercapto-4-methylcoumarin as a reporter of thiol binding to the CdSe quantum dot surface. *Chem. Commun.* **22**, 3202-3204 (2009).
12. Dübner, M., Gevrek, T. N., Sanyal, A., Spencer, N. D., Padeste, C. Fabrication of thiol-ene "Clickable" copolymer-brush nanostructures on polymeric substrates via extreme ultraviolet interference lithography. *ACS Appl. Mater. Interfaces*. **7**, 11337- 11345 (2015).
13. Melo, J. S. De Fernandes, P. F. Spectroscopy and photophysics of 4- and 7-hydroxycoumarins and their thione analogs. *J. Mol. Struct.* **565-566**, 69-78 (2001).
14. Malin, U., Bo, D. Quantum chemical comparison of vertical, adiabatic, and 0-0 excitation energies: The PYP and GFP chromophores. *J. Computational Chem.* **33**, 1892-1901 (2012).
15. Nuttawisit, Y., Khajadpai, T., Vithaya, R. Exploring molecular structures, orbital interactions, intramolecular proton-transfer reaction kinetics, electronic transitions and complexation of 3-hydroxycoumarin species using DFT methods. *J. Molecular Graphics and Modelling,* **51**, 13-26 (2014).
16. Georgieva, I., Trendafilova, N., Aquino, A., Lischka, H. Excited state properties of 7-hydroxy-4-methylcoumarin in the gas phase and in solution. *A Theoretical. Study J. Phys. Chem. A ,***109**, 11860-11869 (2005)
17. Georgieva, I., Trendafilova, N., Aquino, A., Lischka, H. Excited-state proton transfer in 7-hydroxy-4-methylcoumarin along a hydrogen-bonded water wire. *J. Phys. Chem. A,* **111**, 127-135 (2007).
18. Levine, B. G., Chaehyuk, K., Quenneville, J., Martinez, T. J. Conical intersections and double

excitations in time-dependent density functional theory. *J. Molecular. Physics.* **104**, 1039-1051 (2006).

19. Nelson, T., Fernandez-Alberti, S., Roitberg, A. E., Tretiak, S. Electronic delocalization, vibrational dynamics, and energy transfer in organic chromophores. *J. Phys. Chem. Lett.* **8**, 3020-3031 (2017).

20. Crespo-Otero, R., Barbatti, M. Recent advances and perspective on nonadiabatic mixed quantum-classical dynamics. *Chem. Rev.* **118**, 7026-7068 (2018).

21. Domcke, W., Yarkony, D. R., Koeppel, H. (Eds.), "*Conical Intersections, Electronic Structure, Dynamics and Spectroscopy*", World Scientific Publishing Co., (2004).

22. Curchod, B. F., Martínez, T. J. Ab Initio nonadiabatic quantum molecular dynamics. *Chem. Rev.* **118**, 3305-3336 (2018).

23. Subotnik, J. E., Shenv Neil Decoherence and surface hopping, when can averaging over initial conditions help capture the effects of wave packet separation? *The Journal of Chemical Physics,* **134** 244114-1-244114-8 (2011).

24. Spartan, version 18.1.2, Wavefunction, Inc., Irvine, CA, USA (2018).

25. Neese, F. The ORCA program system Wiley interdisciplinary. *Reviews - Computational Molecular Science,* **2**, 73-78 (2012). ORCA, version 4.1.1. Manual at https://orcaforum.kofo.mpg.de/

26. Yanai, T., Tew, D., Handy, N. A new hybrid exchange-correlation functional using the Coulomb-attenuating method (CAM-B3LYP). *Chem. Phys. Lett.* **393**, 51-57 (2004).

27. Neese, F., Wennmohs, F., Hansen, A., Becker, U. Efficient, approximate and parallel Hartree-Fock and hybrid DFT calculations. A 'chain-of-spheres' algorithm for the Hartree-Fock exchange. *Chem. Phys.* **356**, 98-109 (2009).

28. Izsak, R., Neese, F. An overlap fitted chain of spheres exchange method. *J. Chem. Phys.* **135**(14), 144105 (2011)

29. Petrenko, T., Kossmann, S., Neese, F. Efficient time-dependent density functional theory approximations for hybrid density functionals: Analytical gradients and parallelization. *J. Chem. Phys.* **134**, 054116 (2011).

30. Penfold, T. J., Gindensperger, E., Daniel, C., Marian, C. M. Spin-vibronic mechanism for intersystem crossing. *Chem. Rev.* **118**, 6975-7025 (2018).

31. Marx, D., Hutter, J. "*Ab Initio Molecular Dynamics, Basic Theory and Advanced Methods*", Cambridge University Press, UK (2012).

32. Lin, C. Y., George, M. W., Gil, P. M. W. A Density functional for predicting molecular vibrational frequencies. *Aust. J. Chem.* **57**, 365-370 (2004).